

Published in final edited form as:

*Proteins*. 2013 June ; 81(6): 919–925. doi:10.1002/prot.24259.

## Temperature-dependent conformational change affecting Tyr11 and sweetness loops of brazzein

Claudia C. Cornilescu<sup>1</sup>, Gabriel Cornilescu<sup>1</sup>, Hongyu Rao<sup>2</sup>, Sarah F. Porter<sup>2</sup>, Marco Tonelli<sup>1</sup>, Michele L. DeRider<sup>2</sup>, John L. Markley<sup>1,2,\*</sup>, and Fariba M. Assadi-Porter<sup>1,2,\*</sup>

<sup>1</sup>National Magnetic Resonance Facility at Madison, University of Wisconsin-Madison, Wisconsin 53706

<sup>2</sup>Department of Biochemistry, University of Wisconsin-Madison, Wisconsin 53706

### Abstract

The sweet protein brazzein, a member of the Csβα fold family, contains four disulfide bonds that lend a high degree of thermal and pH stability to its structure. Nevertheless, a variable temperature study has revealed that the protein undergoes a local, reversible conformational change between 37 and 3°C with a midpoint about 27°C that changes the orientations and side-chain hydrogen bond partners of Tyr8 and Tyr11. To test the functional significance of this effect, we used NMR saturation transfer to investigate the interaction between brazzein and the amino terminal domain of the sweet receptor subunit T1R2; the results showed a stronger interaction at 7°C than at 37°C. Thus the low temperature conformation, which alters the orientations of two loops known to be critical for the sweetness of brazzein, may represent the bound state of brazzein in the complex with the human sweet receptor.

### Keywords

human sweet receptor; sweet protein; NMR spectroscopy; three-dimensional solution structures; saturation transfer difference spectroscopy

## INTRODUCTION

The high-potency sweet protein brazzein occurs naturally in the fruit from *Pentadiplandra brazzeana* Baillon as two isoforms.<sup>1</sup> The major form (pGlu-brazzein) contains a pyroglutamate (pGlu) residue at its N-terminus, and the minor form (brazzein) lacks that residue. Brazzein has twice the sweetness of pGlu-brazzein.<sup>1</sup> Brazzein activates the primary human sweet taste receptor, a heterodimeric G-protein coupled receptor (GPCR) composed of two subunits, T1R2 and T1R3.<sup>2–5</sup> Brazzein is thought to interact with at least two sites on the human sweet taste receptor.<sup>6</sup> These sites are located in the amino-terminal domain (ATD) of T1R2 and in the cysteine rich domain (CRD) of T1R3.<sup>6</sup> Calcium imaging assays of HEK cells transfected with human T1R2+T1R3 respond to a variety of sweet-tasting compounds including sugars, amino acids, sweet tasting proteins, and synthetic sweeteners.<sup>3,5,7–10</sup> Although known sweet proteins (brazzein, monellin, and thaumatin, and sweet-modifying glycoproteins, such as miraculin and curculin) display low sequence and

structural similarity to one another, it has been proposed that they might share a common mechanism for receptor activation.<sup>11</sup> ‘Wedge’ models<sup>11–14</sup> postulate that sweet proteins dock in the open cleft of either T1R2 or T1R3, despite their large size relative to the dimensions of the cleft.<sup>11,15</sup> Extensive mutagenesis studies of brazzein<sup>6,16,17</sup> have identified three critical surface interaction sites: Site 1 (Loop43), Site 2 (N- and C-termini plus Glu36, and Loop33), and Site 3 (Loop9–19).

Previous studies have indicated that brazzein undergoes a temperature-dependent structural change. Early 1D <sup>1</sup>H NMR studies of brazzein isolated from fruit (primarily pGlu-brazzein)<sup>1</sup> showed that the signals for <sup>1</sup>H<sup>ε1</sup> and <sup>1</sup>H<sup>ε2</sup> of Tyr11 were separate at 22°C but broad and overlapping at 37°C,<sup>18</sup> indicating that the tyrosine ring flips more slowly at the lower temperature. Direct detection of hydrogen bonds by NMR in brazzein at 37 and 10°C showed strengthening of most H-bonds at the lower temperature; however, a structural rearrangement at low temperature led to the loss of two H-bonds located in the middle of the two antiparallel β-strands connecting sweetness Sites 1 and 2 (Glu36 H<sup>N</sup>-Ile48 O, and Ile48 H<sup>N</sup>-Glu36 O) and the appearance of two new H-bonds between Asp40 H<sup>N</sup>-Asn44 O and Asn44 H<sup>N</sup>-Glu41 O<sup>γ</sup> in Loop 43 (Site 1).<sup>19</sup> Here, we report high-resolution structures of brazzein at low (3°C) and high (37°C) temperatures that reveal the nature of the local temperature-dependent conformational change. We further report results from an NMR saturation transfer experiment<sup>6</sup> carried out at 7, 27, and 37°C, which suggest that the low-temperature form of brazzein interacts preferentially with the ATD-T1R2 domain of the human sweet receptor.

## METHODS

<sup>13</sup>C/<sup>15</sup>N labeled brazzein was produced as the SUMO-brazzein fusion, cleaved from the fusion by SUMO protease, and purified by reversed-phase high pressure liquid chromatography as previously described.<sup>20</sup> NMR samples contained 1–2 mM [U-<sup>15</sup>N, U-<sup>13</sup>C]-brazzein in 90% H<sub>2</sub>O/10% <sup>2</sup>H<sub>2</sub>O, with the pH adjusted to 5.2 by adding 0.1N NaOH or 0.1N HCl as needed. Isotropic NMR data were acquired at 37°C from 280 μL samples in a 5 mm Shigemi tube. <sup>15</sup>N-<sup>1</sup>H HSQC, <sup>13</sup>C-<sup>1</sup>H HSQC (aromatic and aliphatic), 3D <sup>15</sup>N-NOESY ( $t_{\text{mix}} = 100$  ms), 3D <sup>13</sup>C-NOESY (aliphatic,  $t_{\text{mix}} = 140$  ms; and aromatic,  $t_{\text{mix}} = 100$  ms) were collected on Varian INOVA 600 or 800 spectrometers equipped with cryogenic probes. Data for H-bond detection were collected on a Bruker DMX500 spectrometer equipped with a triple-resonance cryogenic probe with a  $z$ -gradient.<sup>21</sup> [<sup>15</sup>H-<sup>15</sup>N] HSQC, [<sup>1</sup>H-<sup>13</sup>C] HSQC, HNC0, HNCACB, CBCA(CO)NH, C(CO)NH, H(CCO)NH, H(C)CH-TOCSY, (HB)CB(CGCD)HD, (HB)CB(CGCDCE)HE, 3D <sup>15</sup>N-NOESY ( $t_{\text{mix}} = 100$  ms) and 3D <sup>13</sup>C-NOESY aliphatic ( $t_{\text{mix}} = 100$  ms) and aromatic ( $t_{\text{mix}} = 100$  ms) spectra were collected on Varian VNMRS 600 and 800 spectrometers equipped with cryogenic probes at 3 and 37°C. The same sample was used for the collection of <sup>15</sup>N-<sup>1</sup>H HSQC and <sup>13</sup>C-<sup>1</sup>H HSQC (aliphatic and aromatic) spectra at 37, 32, 27, 22, 17, 12, 7, and 2°C on a Varian INOVA 600 spectrometer equipped with a cryogenic probe. NMRPipe software<sup>22</sup> was used to process and analyze the NMR data. The titrView module in NMRPipe was used to follow the NMR peak position changes during the temperature titration. Structure calculations and refinements made use of the torsion angle molecular dynamics and the internal variable dynamics modules of Xplor-NIH.<sup>23</sup> The TALOS+ program<sup>24</sup> provided pairs of  $\phi/\psi$  backbone torsion angle restraints and identified the secondary structure, which was confirmed by local NOEs. Additionally, broad rotameric restraints were derived from statistics of 100 structures calculated using torsion angle database potentials.<sup>25</sup> The energetically favorable rotameric combinations were deduced from the sterically allowed configurations in the brazzein fold in conjunction with statistics of the database of high-resolution structures used to derive those potentials. Structural statistics of the final structures are shown in Supporting Information Table S1. The unlabeled ATD of the human

sweet taste receptor 2 (ATD-T1R2) was produced by SUMO-fusion and purified by Ni-NTA column chromatography and followed by gel filtration.<sup>20,26</sup> The receptor (50  $\mu$ M) was resuspended in perdeuterated Tris buffered saline: 50 mM Tris.HCl buffer, 150 mM NaCl, and 5% glycerol, 1 mM DTT, 1 mM 2-mercaptoethanol, and 1 mM ZW3-14, pH 8.0. The ligand (2 mg brazzein) was added to the receptor preparation prior to data collection. 1D  $^1$ H saturation transfer difference and control NMR data<sup>26-28</sup> were collected on a Varian 600 MHz spectrometer equipped with a cryogenic probe. In addition, STD signals were monitored as a function of increasing amounts of ligand to detect possible saturation of specific binding. The saturation frequency was set at -1 ppm (on receptor protein signals only). A reference spectrum was acquired on every other scan with the saturation frequency set at 50 ppm (away from the receptor and ligand signals). The two transients were then subtracted in real time to yield the STD spectrum. The experiments were carried out as 1D  $^1$ H experiments with 1024 scans and 1024 complex points as described previously.<sup>27,28</sup> To ensure that the selective receptor irradiation did not excite ligand signals, the same experiment was repeated on a sample containing only ligand and yielded no STD signal.

## RESULTS AND DISCUSSION

We have prepared brazzein labeled uniformly with  $^{13}$ C and  $^{15}$ N and have determined high-resolution NMR solution structures at 3 and 37°C. Comparison of the two solution structures revealed that brazzein undergoes a conformational change at low temperature that affects the positions of both Tyr8 and Tyr11 and locks the Tyr11 ring so that it no longer flips rapidly. This conformational change explains earlier temperature-dependent changes observed in the signals from Tyr11<sup>1</sup> and the hydrogen bonding pattern.<sup>19</sup> Because Tyr8 and Tyr11 are part of Site 3 known to be critical to brazzein sweetness,<sup>6</sup> the two conformational states likely have different binding affinities.

We collected a series of NH-HSQC spectra and aromatic and aliphatic region CH-HSQC spectra as a function of temperature in 5°C steps from 37 to 2°C (Fig. 1 and Supporting Information Fig. S1). These spectra allowed us to trace NMR peak assignments made at 37°C to peaks at 3°C. A standard set of triple resonance experiments served to complete and validate the assignments. This process led to virtually complete (95%) chemical shift assignments at 3°C. The chemical shifts at 37 and 3°C have been deposited at BMRB under accession numbers 16,215 and 18,710, respectively. Examination of the Tyr11 signals in the aromatic  $^{13}$ C-HSQC NMR spectra collected as a function of temperature (Fig. 1) revealed that the protein undergoes a local conformational transition with a midpoint around 27°C. The Tyr11 ring, which undergoes rapid ring flips in the high-temperature conformation, becomes constrained or “locked” and flips slowly in the low-temperature conformation. In addition, the Tyr11 hydroxyl proton ( $^1$ H<sup>o</sup>) becomes visible at low temperatures at a chemical shift (10.13 ppm) typical for H-bonding. Tyr11 occupies different environments in the two conformational states as demonstrated by clearly different NOE contacts (Fig. 2). The environments of the other five Tyr residues appear not to change, because their chemical shifts exhibited little temperature dependence (Supporting Information Fig. S1).

We used heteronuclear  $^1$ H/ $^{13}$ C/ $^{15}$ N NMR data acquired at 37 and 3°C to obtain highly refined three-dimensional structures of brazzein. These structures have been deposited in the PDB under identifiers 2LY5 and 2LY6, respectively. The families of low-energy bundles representing the solution structures at 37 and 3°C had RMSDs of 0.12 and 0.09 Å, respectively. At both temperatures, most of the side chains in the hydrophobic core were highly structured (Supporting Information Fig. S2). A relatively high number of unambiguously assigned NOEs per residue (26.0 for 37°C and 32.5 for 3°C) contributed to the high precision of the final coordinates (Supporting Information Table S1). The backbone

pairwise RMSD between the lowest energy structures at 37 and 3°C was 0.75 Å (Supporting Information Fig. S3).

The temperature-dependent conformational change alters a number of regions of brazzein that have shown to be important for the sweetness of the protein and/or its interaction with the sweet receptor. The N-terminal loop of brazzein (residues 9–19 of Site3) is essential for the sweetness of the protein.<sup>6</sup> The Tyr8Ala variant showed a large decrease in sweetness.<sup>6,16</sup> The insertion of two amino acids (Arg–Ile) between residues Leu18 and Ala19 in loop 9–19 abolished the sweetness of the protein. Mutation of Asp29 (to Lys, Glu, or Ala) resulted in sweeter forms of brazzein.<sup>17</sup>

Close inspection of the lowest energy structures (Fig. 3) allowed identification of putative H-bonds forming at 37°C between Tyr11-O<sup>n</sup>H<sup>n</sup> and Asp29-C<sup>γ</sup>O<sup>δ1</sup> and a bifurcated H-bond between Tyr8-O<sup>n</sup>H<sup>n</sup> and the central Cys26/Cys49 disulfide bond, whereas at 3°C Tyr11-O<sup>n</sup>H<sup>n</sup> participates in H-bonds to Cys47-S<sup>γ</sup> (disulfide bonded to Cys22) and to Tyr8-O<sup>n</sup>H<sup>n</sup>, which is H-bonded to Asp29-C<sup>γ</sup>O<sup>δ1</sup>. Additionally, at 3°C, Glu9-C<sup>δ</sup>O<sup>ε1</sup> anchors to Lys42-N<sup>ζ</sup> through an H-bond. The structure at 3°C is further stabilized by two H-bonds to backbone carbonyls (not present at 37°C): Tyr8-O<sup>n</sup>H<sup>n</sup> to Asp25-CO and Tyr11-H<sup>N</sup> to Glu9-CO. At 3°C, Pro-12 in sweet Site3 repositions toward sweet Site1 (Loop43 region). These changes in H-bonding contribute to the observed difference in the conformation of sweet Site3, which spans residues 9 through 19.<sup>6</sup> The distinct spectral behavior of Tyr11 and Tyr8 is confirmed by close analysis of their structural arrangement: whereas Tyr8 is situated in a solvent accessible pocket at both temperatures, Tyr11 is completely solvent exposed at 37°C but becomes sandwiched between Lys15 and the backbone hydrogen bond between Tyr11-HN and Glu9-CO at 3°C (Fig. 4). This structural detail agrees with the experimental NMR data that suggests ring flip hindrance only for Tyr11 at 3°C.

The hydroxyl oxygen to sulfur distances in the H-bonds described above are less than 3.5 Å in agreement with the mean of  $3.47 \pm 0.22$  Å for a single bifurcated H-bond in a survey of sulfur H-bonds in high-resolution structures deposited in the PDB.<sup>29</sup> These H-bonds may modulate the positions of the two central disulfide bonds (Cys22–Cys47; Cys26–Cys49), which in turn would affect the backbone conformation of the entire protein scaffold. This would explain the quite widespread distribution of the largest amide chemical shift differences between 37°C and 3°C (residues 5, 7, 9, 19, 20, 24, 35, 39, 45, 54). In contrast, the largest side chain carbon chemical shift differences are mainly localized in regions on opposite sides of the protein that correspond to sweet Site1, Arg43(C<sup>β</sup>), Leu45(C<sup>β</sup>, C<sup>δ1</sup>) and sweet Site2, Lys30(C<sup>ε</sup>), Ala32(C<sup>β</sup>), Arg33(C<sup>β</sup>, C<sup>γ</sup>, C<sup>δ</sup>) [Supporting Information Fig. S1(A,B) and Fig. S3].<sup>6</sup>

We used saturation transfer difference NMR (STD-NMR) spectroscopy to monitor the interaction between brazzein and the ATD-T1R2 ligand binding domain of the human sweet receptor at 7, 27, and 37°C (Fig. 5). Our results show specific binding interactions of brazzein at the lowest temperature (7°C) as is apparent by presence of peaks in both the methyl (0.47–0.7 ppm) and aromatic/amide regions (~6.5–7.5 ppm). The methyl peaks in the STD spectrum at 7°C coincide with chemical shifts assigned to Ala32 (H<sup>β</sup>), Leu45 (H<sup>ε1</sup>, H<sup>ε2</sup>), and Ile48 (H<sup>δ1</sup>, H<sup>δ2</sup>) belonging to Sites 1 and 2 in the low-temperature form but not the high-temperature form of brazzein. Ile48 is located in β-strand III and is flanked by two cysteine residues, Cys47 and Cys49 that are disulfide bonded, respectively, to Cys22 and Cys26 in the α-helix. The temperature-dependent changes observed in the chemical shifts of the side chain of Ile48 are consistent with the loss of the H-bond between Ile48 O and Glu36 H<sup>N</sup> at low temperature.<sup>19</sup>

## CONCLUSIONS

Considerable evidence has established the presence of discrete global fluctuations in protein conformation, and a vast majority of data support the conformational selection model (Monod-Wyman-Changeux) of signal transduction.<sup>30</sup> Because the temperature-dependent transition of brazzein affects multiple sites known to be important to its interaction with the heterodimeric sweet receptor or to its sweetness, we hypothesized that the two conformational states interact differentially with the receptor. Results from the STD-NMR binding assay indicate that the low-temperature form of brazzein binds more tightly than the high temperature form to the ATD region of the human T1R2 sweet receptor. It will be of interest to search for protein variants that strongly favor one conformation or the other and to monitor their sweetness and binding interaction with the G-protein coupled human heterodimeric sweet receptor.

## Supplementary Material

Refer to Web version on PubMed Central for supplementary material.

## Acknowledgments

Dedicated to the memory of Prof. Barry Davis, Program Director of the NIH National Institute of Deafness and other Communication Disorders and supporter of innovative ideas and young investigators. The authors thank Dr. Marianna Max for insightful discussions.

Grant sponsor: NIH; Grant number: R01 DC009018, 5P41RR002301-27, RR02301-26S1, 8P41 GM103399-27

## REFERENCES

1. Caldwell JE, Abildgaard F, Dzakula Z, Ming D, Hellekant G, Markley JL. Solution structure of the thermostable sweet-tasting protein brazzein. *Nat Struct Biol.* 1998; 5:427–431. [PubMed: 9628478]
2. Damak S, Rong M, Yasumatsu K, Kokrashvili Z, Varadarajan V, Zou S, Jiang P, Ninomiya Y, Margolskee RF. Detection of sweet and umami taste in the absence of taste receptor T1R3. *Science.* 2003; 301:850–853. [PubMed: 12869700]
3. Nelson G, Hoon MA, Chandrashekar J, Zhang Y, Ryba NJ, Zuker CS. Mammalian sweet taste receptors. *Cell.* 2001; 106:381–390. [PubMed: 11509186]
4. Li X, Staszewski L, Xu H, Durick K, Zoller M, Adler E. Human receptors for sweet and umami taste. *Proc Natl Acad Sci U S A.* 2002; 99:4692–4696. [PubMed: 11917125]
5. Jiang P, Ji Q, Liu Z, Snyder LA, Benard LM, Margolskee RF, Max M. The cysteine-rich region of T1R3 determines responses to intensely sweet proteins. *J Biol Chem.* 2004; 279:45068–45075. [PubMed: 15299024]
6. Assadi-Porter FM, Maillet EL, Radek JT, Quijada J, Markley JL, Max M. Key amino acid residues involved in multi-point binding interactions between Brazzein, a sweet protein, and the T1R2–T1R3 human sweet receptor. *J Mol Biol.* 2010; 398:584–599. [PubMed: 20302879]
7. Nelson G, Chandrashekar J, Hoon MA, Feng L, Zhao G, Ryba NJ, Zuker CS. An amino-acid taste receptor. *Nature.* 2002; 416:199–202. [PubMed: 11894099]
8. Jiang P, Cui M, Zhao B, Liu Z, Snyder LA, Benard LM, Osman R, Margolskee RF, Max M. Lactisole interacts with the transmembrane domains of human T1R3 to inhibit sweet taste. *J Biol Chem.* 2005; 280:15238–15246. [PubMed: 15668251]
9. Jiang P, Cui M, Zhao B, Snyder LA, Benard LM, Osman R, Max M, Margolskee RF. Identification of the cyclamate interaction site within the transmembrane domain of the human sweet taste receptor subunit T1R3. *J Biol Chem.* 2005; 280:34296–34305. [PubMed: 16076846]
10. Xu H, Staszewski L, Tang H, Adler E, Zoller M, Li X. Different functional roles of T1R subunits in the heteromeric taste receptors. *Proc Natl Acad Sci U S A.* 2004; 101:14258–14263. [PubMed: 15353592]

11. Kanehisa M, Goto S, Hattori M, Aoki-Kinoshita KF, Itoh M, Kawashima S, Katayama T, Araki M. From genomics to chemical genomics: new developments in KEGG. *Nucleic Acids Res.* 2006; 34:D354–D357. [PubMed: 16381885]
12. Spadaccini R, Trabucco F, Saviano G, Picone D, Crescenzi O, Tancredi T, Temussi PA. The mechanism of interaction of sweet proteins with the T1R2–T1R3 receptor: evidence from the solution structure of G16A-MNEI. *J Mol Biol.* 2003; 328:683–692. [PubMed: 12706725]
13. Walters DE, Hellekant G. Interactions of the sweet protein brazzein with the sweet taste receptor. *J Agric Food Chem.* 2006; 54:10129–10133. [PubMed: 17177550]
14. Temussi PA. Why are sweet proteins sweet? Interaction of brazzein, monellin and thaumatin with the T1R2–T1R3 receptor. *FEBS Lett.* 2002; 526:1–4. [PubMed: 12208493]
15. Tancredi T, Iijima H, Saviano G, Amodeo P, Temussi PA. Structural determination of the active site of a sweet protein. A 1 H NMR investigation of pMNEI. *FEBS Lett.* 1992; 310:27–30. [PubMed: 1526280]
16. Assadi-Porter FM, Aceti DJ, Markley JL. Sweetness determinant sites of brazzein, a small, heat-stable, sweet-tasting protein. *Arch Biochem Biophys.* 2000; 376:259–265. [PubMed: 10775411]
17. Jin Z, Danilova V, Assadi-Porter FM, Markley JL, Hellekant G. Monkey electrophysiological and human psychophysical responses to mutants of the sweet protein brazzein: delineating brazzein sweetness. *Chem Senses.* 2003; 28:491–498. [PubMed: 12907586]
18. Caldwell JE, Abildgaard F, Ming D, Hellekant G, Markley JL. Complete 1H and partial 13C resonance assignments at 37 and 22 degrees C for brazzein, an intensely sweet protein. *J Biomol NMR.* 1998; 11:231–232. [PubMed: 9679299]
19. Assadi-Porter FM, Abildgaard F, Blad H, Markley JL. Correlation of the sweetness of variants of the protein brazzein with patterns of hydrogen bonds detected by NMR spectroscopy. *J Biol Chem.* 2003; 278:31331–31339. [PubMed: 12732626]
20. Assadi-Porter FM, Patry S, Markley JL. Efficient and rapid protein expression and purification of small high disulfide containing sweet protein brazzein in *E. coli*. *Prot Expr Purif.* 2008; 58:263–268.
21. Cordier F, Grzesiek S. Direct observation of hydrogen bonds in proteins by interresidue  $^3\text{H}_{\text{NC}}$  scalar couplings. *J Am Chem Soc.* 1999; 121:1601–1602.
22. Delaglio F, Grzesiek S, Vuister GW, Zhu G, Pfeifer J, Bax A. NMRPIPE—a multidimensional spectral processing system based on UNIX Pipes. *J Biomol NMR.* 1995; 6:277–293. [PubMed: 8520220]
23. Schwieters CD, Kuszewski JJ, Tjandra N, Clore GM. The Xplor-NIH NMR molecular structure determination package. *J Magn Reson.* 2003; 160:65–73. [PubMed: 12565051]
24. Shen Y, Delaglio F, Cornilescu G, Bax A. TALOS+: a hybrid method for predicting protein backbone torsion angles from NMR chemical shifts. *J Biomol NMR.* 2009; 44:213–223. [PubMed: 19548092]
25. Clore GM, Kuszewski J. Chi(1) rotamer populations and angles of mobile surface side chains are accurately predicted by a torsion angle database potential of mean force. *J Am Chem Soc.* 2002; 124:2866–2867. [PubMed: 11902865]
26. Venkitakrishnan RP, Benard O, Max M, Markley JL, Assadi-Porter FM. Use of NMR saturation transfer difference spectroscopy to study ligand binding to membrane proteins. *Methods Mol Biol.* 2012; 914:47–63. [PubMed: 22976022]
27. Assadi-Porter FM, Tonelli M, Maillet E, Hallenga K, Benard O, Max M, Markley JL. Direct NMR detection of the binding of functional ligands to the human sweet receptor, a heterodimeric family 3 GPCR. *J Am Chem Soc.* 2008; 130:7212–7213. [PubMed: 18481853]
28. Assadi-Porter FM, Tonelli M, Maillet EL, Markley JL, Max M. Interactions between the human sweet-sensing T1R2–T1R3 receptor and sweeteners detected by saturation transfer difference NMR spectroscopy. *Biochim Biophys Acta.* 2010; 1798:82–86. [PubMed: 19664591]
29. Zhou P, Tian F, Lv F, Shang Z. Geometric characteristics of hydrogen bonds involving sulfur atoms in proteins. *Proteins.* 2009; 76:151–163. [PubMed: 19089987]
30. Cui Q, Karplus M. Allostery and cooperativity revisited. *Protein Sci.* 2008; 17:1295–1307. [PubMed: 18560010]

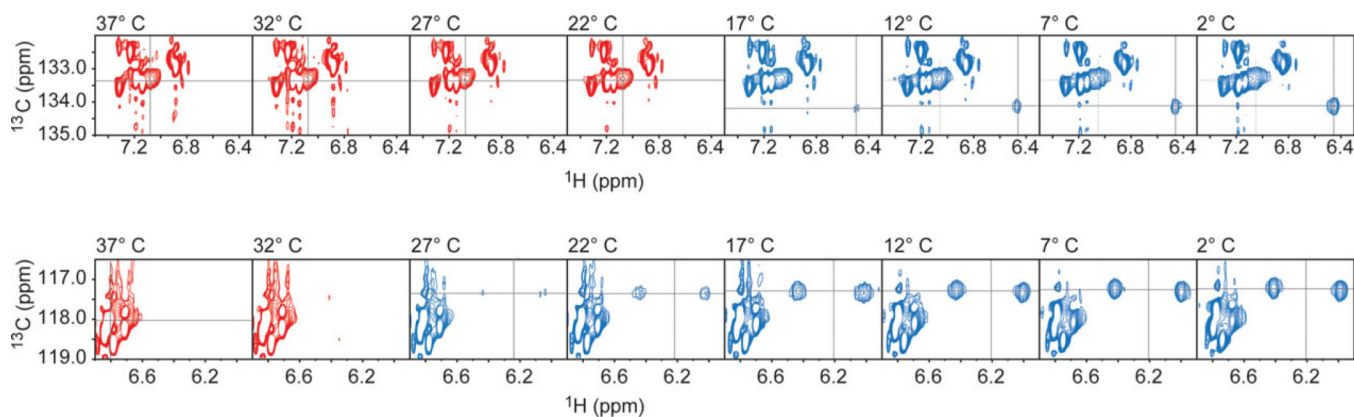


**Figure 1.**

Sections of aromatic  $^{13}\text{C}$ -HSQC NMR spectra of brazzein containing signals from Tyr11 collected at the temperatures indicated. (Upper row) Cross hairs follow the Tyr11  $^{13}\text{C}^{\delta 1}\text{-}^1\text{H}^{\delta 1}$  and  $^{13}\text{C}^{\delta 2}\text{-}^1\text{H}^{\delta 2}$  signals, which yielded single averaged cross peaks as the result of rapid ring flips. The cross peak broadened below the noise level in spectra taken between 32 and 22°C. (Lower row) Cross hairs follow  $^{13}\text{C}^{\epsilon 1}\text{-}^1\text{H}^{\epsilon 1}$  and  $^{13}\text{C}^{\epsilon 2}\text{-}^1\text{H}^{\epsilon 2}$  signals. In the high-temperature conformation, the  $^{13}\text{C}^{\epsilon 1}\text{-}^1\text{H}^{\epsilon 1}$  and  $^{13}\text{C}^{\epsilon 2}\text{-}^1\text{H}^{\epsilon 2}$  signals yielded a single averaged cross peak as the result of rapid ring flips. The signal broadened beyond detection at 32°C, but appeared as two separate peaks at 27°C and below, as indicative of slow ring flips.

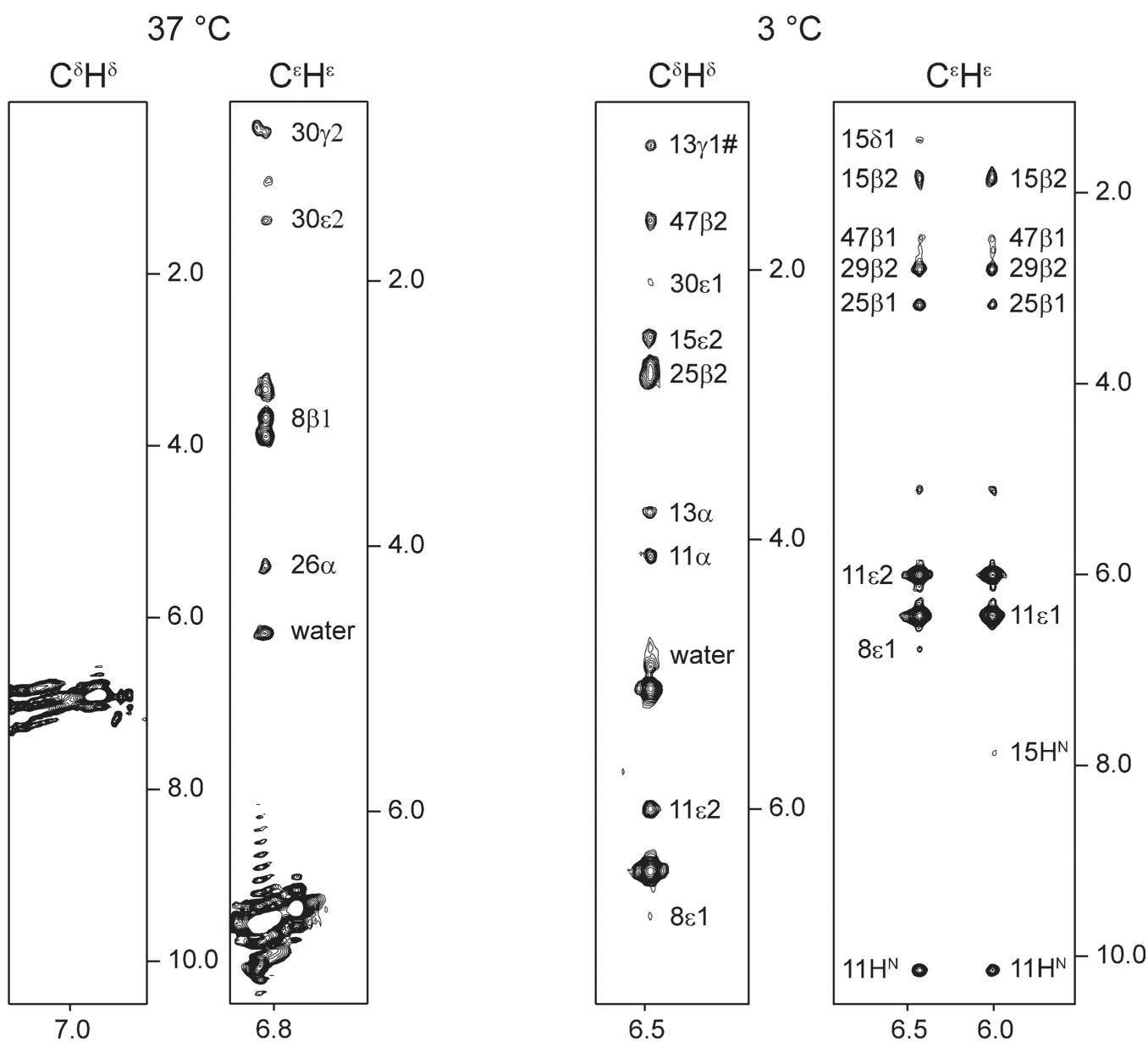


**Figure 2.** Strips from aromatic 3D  $^{13}\text{C}$ -NOESY spectra comparing NOE contacts of the Tyr11  $^1\text{H}^\delta$  and  $^1\text{H}^\epsilon$  protons at (left panels) 37°C and (right panels) 3°C. Unlabeled peaks are either diagonal peaks or belong to other residues.



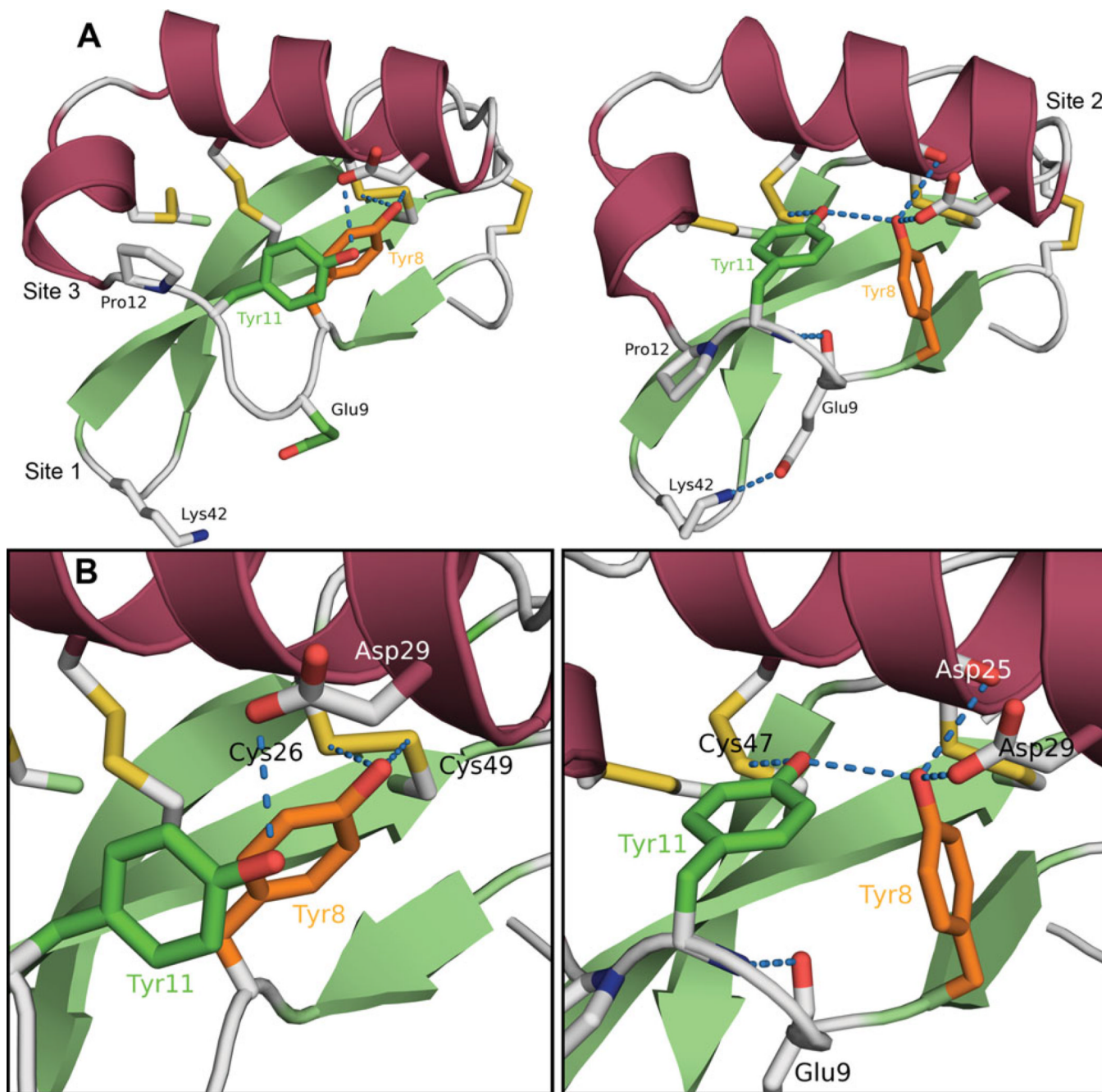


**Figure 3.** Comparison of the structures of brazzein determined at (left panels) 37°C and (right panels) 3°C with Tyr8 in gold and Tyr11 in green. Shown are relevant H-bonds (blue dotted lines) and the side chains of residues that significantly change conformation and/or H-bond partners (Glu9, Pro12, and Lys42). Disulfide bonds are represented in yellow. **(A)** Ribbon diagrams of the lowest energy structures of brazzein. **(B)** Detail showing the H-bond partners of Tyr 8 and Tyr11.

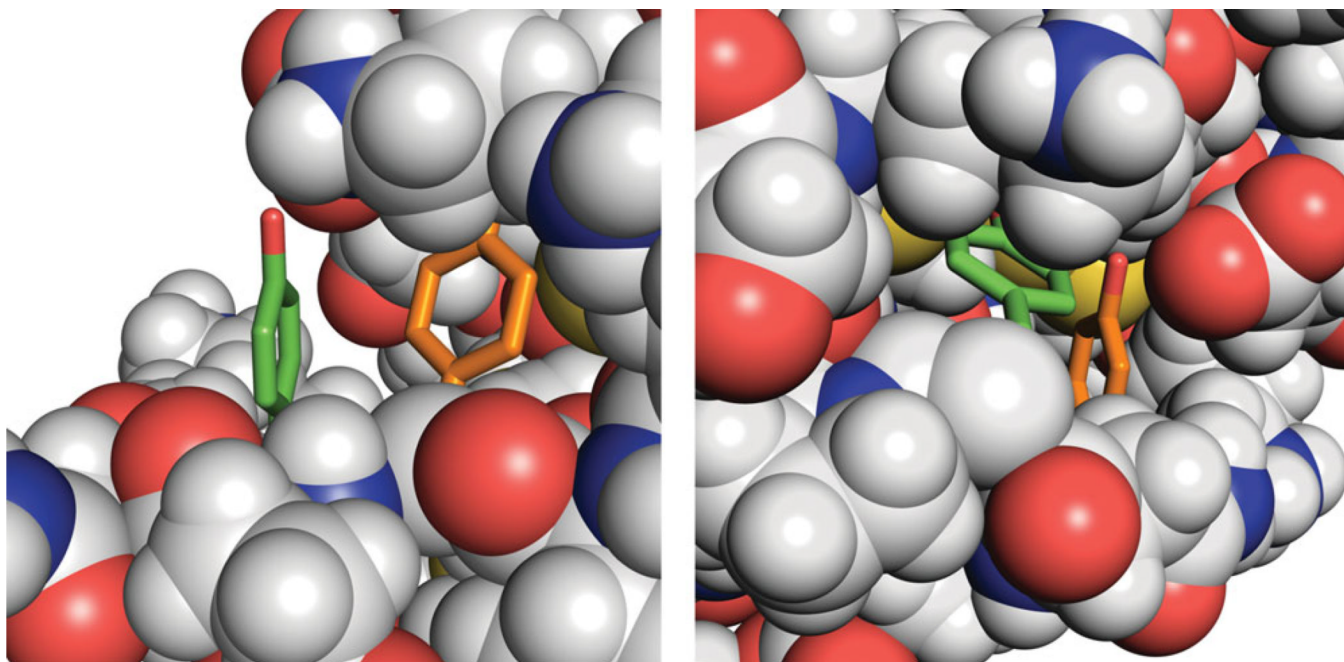


**Figure 4.** Comparison of the environments of Tyr8 in gold and Tyr11 in green in the brazzein structures at (left panel) 37°C and (right panel) 3°C.

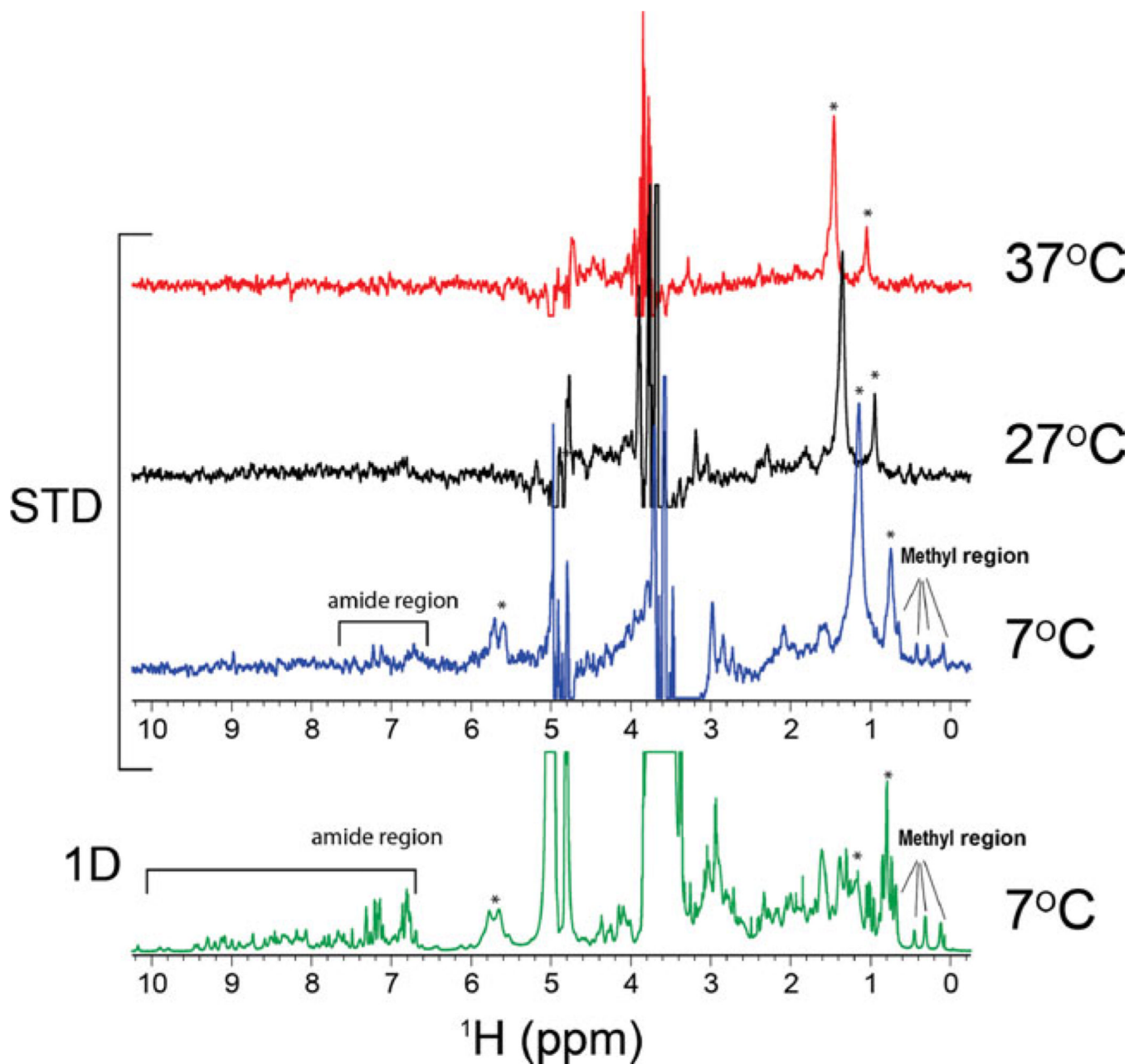


**Figure 5.**

Top: STD spectra of ATD-T1R2 preparations containing brazzein collected at temperatures 37, 27, and 7°C. STD signals of brazzein in the methyl and amide/aromatic regions appearing at 7°C indicate binding to the receptor. Bottom: 1D  $^1\text{H}$  NMR control spectrum of brazzein. Peaks labeled with an asterisk arise from detergent binding to the receptor. Slight changes in peak positions are the result of temperature differences.